Complex Formation between the Hepatitis C Virus Serine Protease and A Synthetic NS4A Cofactor Peptide

Elisabetta Bianchi, Andrea Urbani, Gabriella Biasiol, Mirko Brunetti, Antonello Pessi, Raffaele De Francesco, and Christian Steinkühler*

Istituto di Ricerche di Biologia Molecolare "P. Angeletti" Pomezia, 00040 Rome, Italy

Received December 27, 1996; Revised Manuscript Received April 22, 1997[⊗]

ABSTRACT: The NS3 protein of the hepatitis C virus contains a serine protease that, upon binding to its cofactor, NS4A, is responsible for maturational cleavages that occur in the nonstructural region of the viral polyprotein. We have studied in vitro complex formation between the NS3 protease domain expressed in *Escherichia coli* and a synthetic peptide spanning the minimal domain of the NS4A cofactor. Complex dissociation constants in the low micromolar range were measured using different techniques such as activity titration, fluorescence titration, and pre-equilibrium analysis of complex formation. Cofactor binding was strictly dependent on the glycerol content of buffer solutions and was not significantly influenced by substrate saturation of the enzyme. NS4A peptide binding to NS3 was accompanied by changes in the circular dichroism spectrum in the region between 270 and 290 nm, as well as by an enhancement of tryptophan fluorescence. Conversely, no changes in the far UV region of the circular dichroism spectrum were detectable. These data are indicative of induced tertiary structure changes and suggest that the secondary structure content of the uncomplexed enzyme does not differ significantly from that of the NS3−cofactor complex. Pre-equilibrium measurements of complex formation showed very low values for k_{on}, suggesting conformational transitions to be rate limiting for the association reaction.

The N-terminal third of the hepatitis C virus (HCV)[1] NS3 protein contains a chymotrypsin-like serine protease that performs four out of the five processing events that take place during maturation of the nonstructural portion of the HCV polyprotein (Tomei et al., 1993; Grakoui et al., 1993; Bartenschlager et al., 1993; Eckard et al. 1993; Hijikata et al., 1993; Komoda et al., 1994). Besides, the protease domain at its N-terminus NS3 also contains an RNA helicase domain at its C-terminus. It has been shown that this latter domain is dispensable for optimum protease activity (Failla et al., 1995). For this reason, many groups have focused on the expression and purification of a protein of about 20 kD encompassing only the NS3 protease domain from heterologous expression systems (Suzuki et al., 1995; Shoji et al., 1995; Mori et al., 1996; Butkiewcz et al., 1996). We have recently described the purification and characterization of the enzymatic activity of this truncated protein (Steinkühler et al., 1996a,b).

In vivo, NS3 is a heterodimer consisting of a complex between the protease itself and the viral protein NS4A. The latter is a 54 residue protein that has been shown to bind to the N-terminal region of the protease *via* a central hydrophobic domain spanning residues 21−34 (Failla et al., 1994; Lin et al., 1994, 1995; Failla et al., 1995; Tamji et al., 1995, Satoh et al., 1995; Bartenschlager et al., 1995). NS4A acts as a cofactor of the protease enhancing cleavage at all sites and being an absolute requirement for *in vivo* processing of the NS4B/NS5A junction (Failla et al., 1994). Several studies have shown that a peptide encompassing the central hydrophobic domain of NS4A is sufficient to elicit full activation of the protease (Lin et al., 1995; Tomei et al., 1996; Shimidzu et al., 1996; Koch et al., 1996; Steinkühler et al., 1996a; Butkiewcz et al., 1996). Recently, we have investigated the effects of complex formation with an NS4A based peptide on the cleavage kinetics of NS3 using peptide substrates (Urbani et al., 1997). Monitoring enzymatic activity, it was possible to demonstrate that the degree of activity enhancement experienced by the protease upon binding to Pep4A is both a function of buffer composition and of the sequence of the substrate peptide. This latter finding implies that NS4A influences the mechanism of substrate recognition. Also, some physicochemical requirements of the protease change upon complex formation with the cofactor peptide. Thus, NS3 is competitively inhibited by NaCl (Steinkühler et al., 1996a). This susceptibility to salt inhibition changes quantitatively in the NS3−Pep4A complex, suggesting that substrates may experience different binding modes in free NS3 and in the complex with the cofactor.

Single amino acid substitutions introduced into a wild-type minimum peptide have demonstrated the importance of several residues such as Val-23, Val-24, Ile-25, Val-26, Gly-27, Arg-28, Ile-29, and Leu-31 in establishing contacts necessary for complex formation (Shimidzu et al., 1996; Butkiewcz et al., 1996). These data are suggestive of extensive, multiple contacts between the protease and Pep4A. The recently published three-dimensional structures of the free protease domain (Love et al., 1996) and of the enzyme

* To whom correspondence should be addressed: IRBM, Via Pontina K_m 30, 600 -00040-Pomezia, Italy. Phone: ++39 6 91093232. Fax: ++39 6 91093225. E-mail: Steinkuhler@IRBM.it.

[⊗] Abstract published in *Advance ACS Abstracts,* June 1, 1997.

[1] Abbreviations: Abu, alpha aminobutyric acid; CHAPS, 3-[(3-cholamidopropyl)dimethylammonio]-1-propanesulfonate; cmc, critical micelle concentration; DABCYL, 4-[[4′-(dimethylamino)phenyl]azo]-benzoic acid; DTT, dithiothreitol; EDANS, 5-[(2′-aminoethyl)amino]-naphthalenesulfonic acid; Fmoc, 9-fluorenylmethyloxycarbonyl; HCV, hepatitis C virus; HPLC, high-performance liquid chromatography; NS, nonstructural; TFA, trifluoracetic acid.

S0006-2960(96)03147-9 CCC: $14.00

complexed to an NS4A-derived peptide (Kim et al., 1996) have shed much light on the nature of the interaction between the enzyme and its cofactor. In the structure of the complex, the cofactor peptide intercalates within a β-sheet of the enzyme core actually forming an integral structural component of the protease. In the absence of the NS4A peptide, the N-terminus of the protease, which in the complex forms an antiparallel β-sheet with the cofactor, adopts an open conformation, contacting exposed hydrophobic patches on adjacent molecules in the asymmetric unit.

In the present work we have investigated the formation of a complex between NS3 and its peptide cofactor by monitoring changes in enzymatic activity and the spectroscopic properties of the enzyme as a function of the physicochemical environment. We show that complex formation is absolutely dependent on the presence of glycerol in the buffer and does not cause changes in the protein's secondary structure. Changes in the tertiary structure can instead be measured by perturbations of the environment of the tryptophan residues of the protein. Pre-equilibrium association kinetics show very slow on-rates of complex formation, suggesting that conformational rearrangements must occur in order to accomodate the NS4A peptide into its binding site. The results are discussed in the light of the published three-dimensional structures.

MATERIALS AND METHODS

Enzyme Preparation. *E. coli* BL21(DE3) cells were transformed with a plasmid containing the cDNA coding for the serine protease domain of the HCV BK strain NS3 protein (amino acids 1−180) under the control of the bacteriophage T7 gene 10 promoter. Details of plasmid construction will be published elsewhere. The protease domain was purified as previously described (Steinkühler et al., 1996a). The enzyme was homogeneous as judged from silver stained SDS−PAGE and >95% pure as judged from reversed phase HPLC performed using a 4.6 × 250 mm Vydac C4 column. Enzyme preparations were routinely checked by mass spectrometry done on HPLC-purified samples using a Perkin-Elmer API 100 instrument and N-terminal sequence analysis carried out using Edman degradation on an Applied Biosystems model 470A gas-phase sequencer. Both techniques indicated that in more than 90% of the enzyme molecules the N-terminal methionine and alanine had been removed, yielding an enzyme starting with Pro 2. Enzyme stocks were quantitated by amino acid analysis, shock-frozen in liquid nitrogen, and kept in aliquots at −80 °C until use. Control experiments had shown that this freezing procedure does not affect the specific activity of the enzyme.

Peptides and HPLC Assays. Peptide synthesis was performed by Fmoc/t-Bu chemistry. Protecting groups were as follows: N^{α}(Fmoc), Asp(O-*t*-Bu), Glu(O-*t*-Bu), Lys(Boc), Tyr(*t*-Bu), Ser(*t*-Bu), Thr(*t*-Bu), His(Trt), and Cys(Trt). All amino acids were activated by benzotriazol-1-yloxytris-(pyrrolidino)phosphonium hexafluorophosphate, *N*-hydroxybenzotriazole, and diisopropylethylamine. All peptides were assembled on a Tentagel R RAM resin, yielding peptide amides upon cleavage with TFA 88%, phenol 5%, triisopropylsilane 2%, and water 5%.

Crude peptides were purified by reversed phase HPLC on a Nucleosyl C18, 250 × 21 mm, 100 Å, 7 μm, using H_2O, 0.1% TFA and acetonitrile, and 0.1% TFA as eluents. Analytical HPLC was performed on a Ultrasphere C18, 250 × 4.6 mm, 80 Å, 5 μm (Beckman). Purified peptides were characterized by mass spectrometry and amino acid analysis. The synthesis of the fluorogenic ester substrate, S2, having the sequence Ac-DED(Edans)EEAbuΨ[COO]ASK(Dabcyl)-NH_2, has been previously reported (Taliani et al., 1996).

Concentration of stock solutions of peptides, prepared in DMSO or in buffered aqueous solutions and kept at −80 °C until use, was determined by quantitative amino acid analysis performed on HCl-hydrolyzed samples.

If not specified differently, cleavage assays were performed in 57 μL of 50 mM Tris, pH 7.5, 2% CHAPS, 50% glycerol, and 10 mM DTT (buffer A), to which 3 μL of substrate peptide S1, having the sequence Ac-DEMEE-CASHLPYK-NH_2, were added. Six duplicate data points at substrate concentrations between 15 and 400 μM were used to calculate kinetic parameters. As protease cofactor, we used peptides spanning the central hydrophobic core (residues 21−34) of the NS4A protein. The NS4A-derived peptides Pep4A GSVVIVGRIILSGR-NH_2 or Pep4AK (KKKGSVVIVGRIILSGR-NH_2) were preincubated for 10 min with 10−50 nM protease, and reactions were started by addition of substrate. NS4A peptide concentrations were varied between 0.2 and 25 μM, and eight duplicate data points were determined. Incubation times were chosen in order to obtain <8% substrate conversion. Reactions were stopped by addition of 40 μL of 1% TFA. Cleavage of peptide substrates was determined by HPLC using a Merck-Hitachi chromatograph equipped with an autosampler. Samples of 80 μL were injected on a Lichrospher C18 reversed phase cartridge column (4 × 75mm, 5 μm, Merck), and fragments were separated using a 10−40% acetonitrile gradient at 5%/min using a flow rate of 2.5 mL/min. Peak detection was accomplished by monitoring both the absorbance at 220 nm and tyrosine fluorescence (λ_{ex} = 260 nm, λ_{em} = 305 nm) for substrate S1, while cleavage of the ester substrate S2 was monitored following the fluorescence of the EDANS fluorophore (λ_{ex} = 355 nm, λ_{em} = 495 nm).

Cleavage products were quantitated by integration of chromatograms with respect to appropriate standards. Initial rates of cleavage were determined on samples having <8% substrate conversion. Kinetic parameters were calculated from nonlinear least-squares fit of initial rates as a function of substrate concentration with the help of a Kaleidagraph software, assuming Michaelis−Menten kinetics.

Kinetic determination of K_d values was performed at 10−160 μM S1 substrate concentration and 20−50 nM enzyme. K_d values were calculated by nonlinear least-squares fitting of eq 1 to the data points:

$$V = V_0 + (V_{max}[\text{Pep4AK}])/(K_d + [\text{Pep4AK}]) \quad (1)$$

with V_0 being the velocity in the absence of the cofactor, V being the initial velocity of enzymatic catalysis at a given Pep4AK concentration, V_{max} the velocity at Pep4AK saturation, and K_d the dissociation constant of the NS3−Pep4AK complex.

Circular Dichroism Spectroscopy. Circular dichroism measurements were performed using a Jasco 710 spectropolarimeter equipped with a cell holder thermostatically controlled by a circulating water bath. Spectra were collected at 15 °C by using rectangular quartz cells of 1 cm path length for the near-UV region (320−250 nm) and 0.01 cm path length for the far-UV region (250−190 nm). The measure-

ments were recorded with a 16- s time constant and a 2 nm/min scan speed. Protein concentration was 1 mg/mL for both far- and near-UV regions. The concentration of the samples was determined by quantitative amino acid analysis. Mean residue ellipticity [Ø] was calculated according to

$$[Ø] = Ø100/lc \quad (2)$$

where Ø is the measured ellipticity at a certain wavelength, l is the cell path length in centimeters, and c is the protein concentration in residue moles per liter; the mean residue weight for the protein is MRW = 106 for NS3. Protein solutions were prepared in sodium phosphate buffer 50 mM, pH 7.5, 3 mM DTT, and different concentrations of CHAPS and glycerol. Estimation of the secondary structure content was carried out by using the program K2d for the data between 240 and 200 nm (Andrade et al., 1993). The titration experiment in the near-UV was performed by preincubating 60 μM protease at increasing amounts of Pep4AK for 10 min at 15 °C. The titration curve, which is accompanied by a decrease in ellipticity in the near-UV, was monitored by following the ellipticity at 290 nm as a function of Pep4AK concentration.

Fluorescence Measurements. Fluorescence emission spectra were recorded on a Perkin-Elmer LS50B instrument with a cuvette holder thermostatted at 20 °C. Excitation was at 295 nm, and emission was recorded between 300 and 400 nm at a scan speed of 60 nm/min. Emission and excitation slits were opened to 5 nm. Spectra were routinely corrected for the background signal of buffer and for dilution effects. Titration experiments were performed by pre-equilibrating 800 nM protease for 10 min in 2.5 mL of buffer A. Spectra were recorded before and after addition of Pep4AK. Duplicate determinations were made for each titration point. For each determination, a fresh enzyme solution was used to avoid time-dependent changes in the complex. Dissociation constants were calculated from fluorescence data by fitting expression 3 to the data:

$$\Delta F = (\Delta F_{max}\text{Pep4AK})/(K_d + \text{Pep4AK}) \quad (3)$$

where ΔF is the fluorescence increase at 334 nm induced by a given concentration of Pep4AK and ΔF_{max} is the fluorescence increase observed at enzyme saturation.

Progress Curve Analysis. To determine association rates of Pep4AK with the protease, progress curves were recorded using substrate S2. To this purpose, 25 nM enzyme was preincubated in 2.5 mL buffer A in a thermostatted fluorescence cuvette at 20 °C for 5 min. Solutions were continuously stirred. Reactions were started by addition of 19.2 μM substrate S2 and, in addition to automatic stirring, manually mixed for 5 s. This procedure was required in order to obtain thorough mixing of all components in the presence of 50% glycerol. Substrate S2, being an ester substrate, shows burst kinetics at incubation times that are within the dead time of our mixing procedure. However, in order to ascertain that steady-state conditions have been actually reached, Pep4AK was only added (following the same procedure described above) after verification that a constant velocity had been attained (usually after 40−60 s). Progress curves for activation of the NS3 protease were fitted by nonlinear least-squares analysis to the integrated expression

$$F_t = V_f t + (V_0 - V_f)[1 - \exp(-k_{obs}t)]/k_{obs} + F_i \quad (4)$$

where F_t is the fluorescence at time t, V_f is the final steady state velocity, V_0 is the initial velocity in the absence of cofactor at $t = 0$, k_{obs} is the first-order rate constant for the approach to steady state, and F_i is the initial displacement of F_t from zero at $t = 0$. This equation has been derived to describe the inhibition by slow binding inhibitors (Williams & Morrison, 1979; Morrison, 1982; Cha, 1972) whose kinetic behavior is formally identical to that of a slow binding activator. In the former case, $V_0 > V_f$, yielding a concave-down curve, whereas in the presence of an activator, $V_0 < V_f$. In this latter case, expression 4 would describe a concave-up curve. Expression 4 is based on the assumption that steady-state conditions are applicable to the enzyme−substrate interaction. Therefore, it was demonstrated in independent control experiments that the values for V_0 and V_f were the true steady-state velocities and that no time-dependent deviation from linearity was detectable. It was calculated that substrate depletion was <25% during the experiment.

The second order association rate constant k_{on} is related to k_{obs} by the expression

$$k_{obs} = k_{off} + k_{on}[\text{Pep4AK}] \quad (5)$$

with k_{off} being the first-order dissociation rate constant of the NS3−Pep4AK complex. k_{on} was calculated from the slope of a secondary plot of k_{obs} versus Pep4AK concentration by linear regression analysis. k_{off} was also calculated from this plot as intercept of the linear regression curve with the y-axis. Alternatively, k_{off} was calculated after preformation of an NS3−Pep4AK complex at 2 μM protease + 20 μM Pep4AK for 20 s at 20 °C in buffer A. Under vigorous stirring 25 μL of complex was then diluted directly into the fluorescence cuvette containing 19.2 μM substrate S2 in 2.5 mL buffer A. Progress curves were monitored over a time period of 700 s, and instantaneous velocities were calculated at 10−20 time points along the progress curve. The resulting data were fitted to the expression

$$V_t = V_f[\exp(-k_{off}t)] + V_i \quad (6)$$

where V_t is the instantaneous velocity at a given time t, V_f is the velocity attained when the enzyme−activator complex is fully dissociated, and V_i is the initial, near-zero velocity.

RESULTS

The study of complex formation between NS3 and Pep4A was complicated by the low solubility of the 14-mer 4A-peptide. As a matter of fact, upon addition of Pep4A to solutions of NS3 protease, insoluble NS3−Pep4A complexes could be detected using high-speed centrifugation (not shown). This insoluble material was detectable even at nanomolar protease concentrations. Furthermore, changes in the CD spectrum of Pep4A, indicative of aggregate formation, could be monitored at peptide concentrations above 100 μM (Tomei et al., 1995). These findings prompted us to explore the solubilizing effect of the addition of a stretch of three lysine residues to the N-terminus of Pep4A. This approach has already proven successfull both for peptides and small proteins, the lysine tail yielding much improved solubility without any perturbation of activity and folding (Bianchi et al., 1994). Indeed, the resulting peptide, Pep4AK, showed significantly improved solubility. Moreover, using this peptide, no aggregates could be detected upon

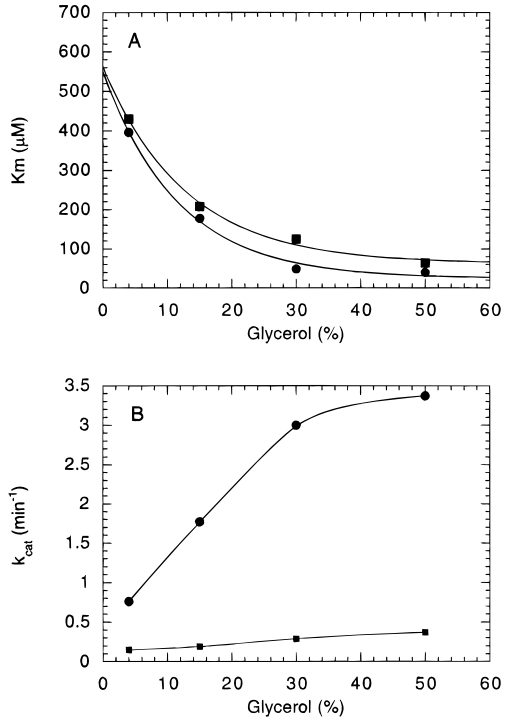

FIGURE 1: Dependence of K_m and k_{cat} on glycerol concentration. NS3 protease (50 nM) was incubated in 50 mM Tris, pH 7.5, 2% CHAPS, 30 mM DTT, and variable glycerol concentrations in the absence (squares) or in the presence (circles) of 16 μM Pep4AK. After 10 min at 23 °C, the reaction was started by addition of 10−300 μM substrate S1. Samples were subsequently analyzed by HPLC. For K_m (A) and k_{cat} (B) determination, initial velocities were calculated at <8% substrate conversion. Kinetic parameters were determined at any single glycerol concentration by fitting the Michaelis−Menten equation to six duplicate data points.

complex formation with the protease in centrifugation experiments, and no concentration-dependent alterations in the CD spectrum were detectable at peptide concentrations as high as 1 mM. As a result of these properties, Pep4AK was also found to activate the NS3 protease more than its nontagged counterpart. In light of these findings, we selected Pep4AK to study complex formation with the NS3 protease. A similar strategy was used by Kim et al. (1996) who crystallized the complex between NS3 and a synthetic 4A peptide modified with the addition of two lysines at both the N- and C-terminus.

Effects of Complex Formation on Enzymatic Catalysis. Previous work has shown that glycerol and detergents enhance the activity of the NS3 protease (Steinkühler et al., 1996a). Using a peptide substrate based on the NS4AB sequence (substrate S1), we explored the combined effects of glycerol, Pep4AK, and the detergent CHAPS on the kinetic parameters K_m and k_{cat}. Glycerol caused both an increase in k_{cat} as well as a decrease in the K_m for substrate S1 (Figure 1). These effects were observed both in the absence and in the presence of Pep4AK. However, the glycerol-dependence curve of k_{cat} was much steeper in the presence of the cofactor than in its absence, whereas no such Pep4AK dependence could be detected monitoring the glycerol effect on K_m. CHAPS on the other hand, had no appreciable effect on K_m but steadily increased k_{cat} in the absence of Pep4AK (not shown). In the presence of the cofactor, an increase in k_{cat} could be monitored going from 0 to 0.1% CHAPS, after which a plateau was reached (not shown).

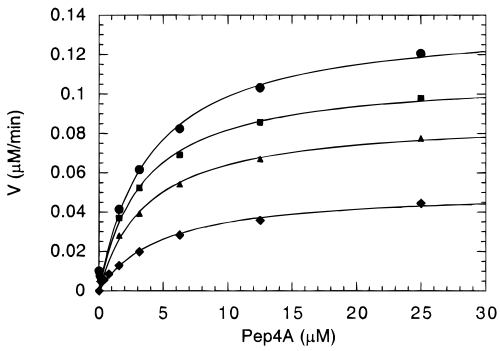

FIGURE 2: Kinetic determination of the dissociation constant of the NS3−Pep4AK complex. NS3 protease (50 nM) was incubated in 50 mM Tris, pH 7.5, 2% CHAPS, 30 mM DTT, and 50% glycerol in the presence of increasing amounts of Pep4AK. Reactions were started by addition of different amounts of substrate S1. After HPLC analysis, K_d values were determined by fitting eq 1 to the data. No significant dependence of the K_d value on substrate concentration could be detected: K_d values of 5.3, 5.3, 4.7, and 4.6 μM were obtained in the presence of 10, 40, 80, and 160 μM substrate S1, respectively.

Table 1: Effect of Glycerol and CHAPS on the Dissociation Constant of the NS3-Pep4AK Complex[a]

glycerol	CHAPS	K_d (μM)
50%	2%	5.3
25%	2%	58
10%	2%	>100
4%	2%	>1000
50%	0.1%	9
50%	0%	31

[a] Dissociation constants were determined kinetically as described in the Materials and Methods. Assays were performed in 50 mM Tris, pH 7.5, 30 mM DTT, and variable concentrations of CHAPS and glycerol. Protease concentrations were 20−50 nM. After addition of Pep4AK, samples were preincubated for 10 min at 23 °C, after which the reaction was started by addition of 40 μM substrate. Reactions were stopped by addition of TFA, and samples were analyzed by HPLC.

The Pep4AK dependence of enzymatic activity was used to determine the dissociation constant of the NS3−Pep4AK complex under optimized assay conditions (50% glycerol and 2% CHAPS). From the titration curves in Figure 2, we calculated K_d = 5.3 μM at [S1] = K_m. Under our experimental conditions, this value actually reflects the affinity of Pep4AK for a mixed population of free enzyme and enzyme−substrate complex. The exact amount of these species depends on the S1:K_m ratio and is thus related to the substrate concentration used to detect enzymatic activity. In order to determine whether free NS3 and the NS3−S1 complex have different affinities for Pep4AK, titration experiments were repeated at different substrate concentrations ranging from 10 μM (K_m/4) to 160 μM (4K_m) (Figure 2). Fitting of eq 1 to the titration data yielded only marginal differences in the K_d values as a function of substrate saturation, indicating that the NS3−S1 complex has, within the experimental error, the same affinity for the cofactor Pep4AK as the free enzyme.

Activity titration experiments were also repeated using different glycerol and CHAPS concentrations (Table 1). The affinity of the protease for the Pep4AK cofactor turned out to be strictly dependent on the glycerol concentration used in the buffer system, becoming actually undetectable at glycerol concentrations below 10%. Also, omission of detergent apparently affected Pep4AK binding (Table 1). In this case, however, optimum binding was restored at

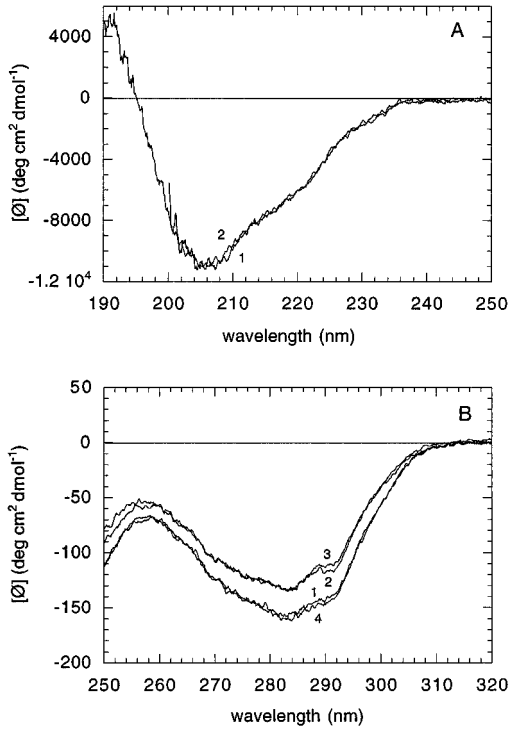

FIGURE 3: Far (A) and near-UV (B) circular dichroism spectra of NS3 at 1 mg/mL at 15 °C in phosphate buffer, 50 mM, pH 7.5, 3 mM DTT, and different glycerol and CHAPS concentrations: (1) 50% glycerol, 2% CHAPS; (2) 5% glycerol, 0.1% CHAPS; (3) 5% glycerol, 2% CHAPS; and (4) 50% glycerol, 0.1% CHAPS.

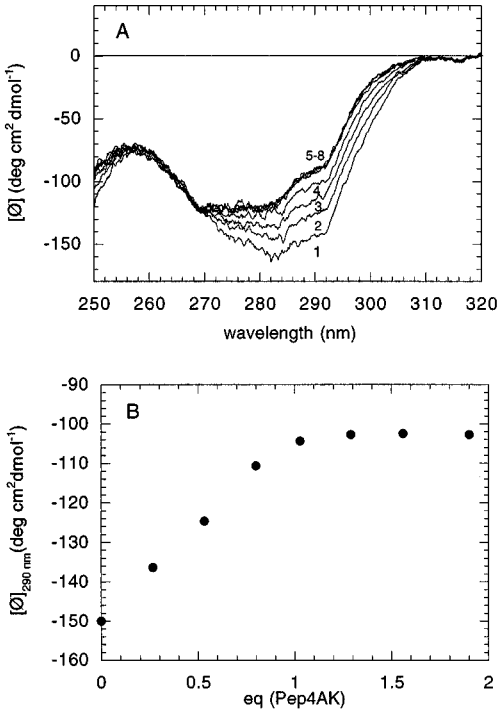

FIGURE 4: Pep4AK-induced conformational change of NS3 as detected by near-UV CD in 50% glycerol, 2% CHAPS, 3 mM DTT, phosphate buffer 50 mM, pH 7.5. (A) CD spectra of NS3 at 60 μM and increasing amount of Pep4AK: (1) 0 equiv, (2) 0.27 equiv, (3) 0.53 equiv, (4) 0.8 equiv, (5) 1.03 equiv, (6) 1.29 equiv, (7) 1.56 equiv, (8) 1.9 equiv. (B) Pep4AK titration of the near-UV CD at 290 nm for NS3.

relatively low detergent concentrations (around 0.1%), well below the cmc value of CHAPS (around 0.5%).

In the following, we explored whether spectroscopically detectable conformational changes could be correlated with the kinetic effects observed upon formation of the NS3−Pep4AK complex.

CD Spectroscopy. Figure 3A shows the far-UV CD spectra of purified NS3 in 50% glycerol, 2% CHAPS, and 50 mM phosphate buffer, pH 7.5, and in 5% glycerol, 0.1% CHAPS, and 50 mM phosphate buffer, pH 7.5. The spectra are superimposable in the region accessible for both solvents, suggesting that neither glycerol nor CHAPS affect secondary structure content. The estimation of secondary structure was determined with the program K2d (Andrade et al., 1994) and gave 10% α-helix, 38% β-structure, and 52% other structures.

The near-UV CD of NS3 is on the contrary strongly dependent on the medium. Spectral changes in this region indicate changes in the asymmetric environment of aromatic residues and disulfide bonds, therefore reflecting changes in the tertiary or the quaternary structure of the protein (Woody, 1995; Kahn, 1979). In Figure 3B, the effect of different concentrations of glycerol and CHAPS is shown. While spectra obtained at 0.1 and 2% CHAPS show only very slight but reproducible differences in the region around 290 nm, the effect of glycerol is much more pronounced, producing an overall increase of the intensity of the spectrum. These spectral changes are expected to reflect changes in the packing of the side chains of the protease. We can rule out the possibility of the formation of oligomers or higher aggregates in these conditions from high-speed centrifugation studies (not shown).

The interaction of NS3 with Pep4AK was studied by monitoring the spectra in both the far- and the near-UV region. A comparative analysis of the far-UV CD of NS3 in the absence of and complexed with Pep4AK reveals that there is no effect on secondary structure upon complex formation (not shown). The far-UV CD spectrum of the complex is in fact superimposable on the sum of the individual spectra of NS3 and Pep4AK. It is noteworthy that the CD contribution of the peptide itself in 50% glycerol and 2% CHAPS is already β as it would be expected to be also in the complex.

The effect of the titration of NS3 with increasing amounts of Pep4AK in the near-UV region is shown in Figure 4. The formation of the complex was followed in 50% glycerol, 2% CHAPS, 3 mM DTT, and 50 mM phosphate buffer, pH 7.5, at a protein concentration of 60 μM. Under these conditions, the addition of Pep4AK produces a large change in the near-UV spectrum, with a decrease of ellipticity, especially in the region between 270 and 290 nm which is dominated by the signals arising from the aromatic side chains, namely two tryptophans and five tyrosines in NS3 (Kahn, 1979; Strickland, 1974). In fact, there is no direct contribution in this spectral region by Pep4AK as it contains no aromatic residues in the sequence. The observed change should be interpreted as due to local alterations of the environment of the side chains, since no change in the global fold of the protein is suggested by the far-UV CD. By monitoring the ellipticity at 290 nm as a function of Pep4AK concentration, we could derive a stoichiometry of 1:1 for the complex between NS3 and Pep4AK (Figure 4B). The change in the near-UV CD upon complex formation was found to be strictly dependent on glycerol concentration (data not shown).

Fluorescence Spectroscopy. Addition of Pep4AK to the NS3 protease resulted in an increase in tryptophan fluorescence with a concomitant blue shift of the fluorescence maximum from 338 to 334 nm (Figure 5). These changes

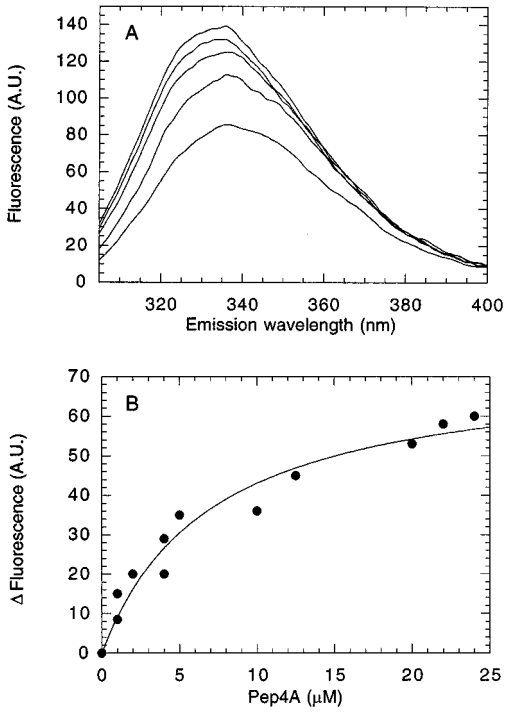

FIGURE 5: (A) Fluorescence emission spectra of NS3 protease in the presence of increasing amounts of Pep4AK. NS3 protease (800 nM) was incubated at 20 °C in 50 mM Tris, pH 7.5, 3 mM DTT, 2% CHAPS, and 50% glycerol. Fluorescence emission spectra were recorded between 305 and 400 nm after excitation at 295 nm in the absence and in the presence of 3, 12, 20, and 24 μM Pep4AK. Spectra were corrected for buffer background and dilution effects. (B) Plot of ΔF versus Pep4AK concentration. The fluorescence increase at 334 nm obtained upon addition of increasing amounts of Pep4AK was plotted against the Pep4AK concentration. Equation 3 was fitted to the data, and the dissociation constant of the Pep4AK−NS3 complex was calculated from the fit. We obtained $K_d = 6.8$ μM.

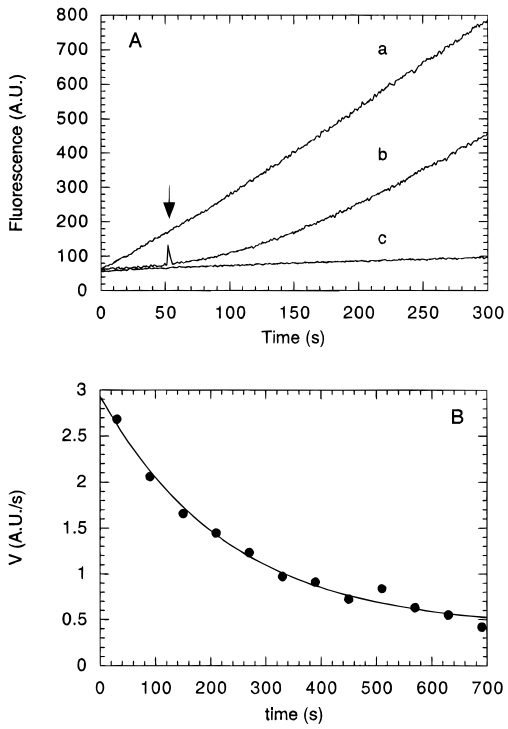

FIGURE 6: (A) Progress curves for activation of NS3 by Pep4AK. Progress curves were recorded in the presence of 19.2 μM fluorogenic ester substrate S2 after 10 min preincubation with 20 μM Pep4AK (curve a) and in the absence of cofactor (curve c). In curve b, 20 μM Pep4AK was added after 50 s. The time point of addition is indicated by the arrow. (B) Determination of the dissociation rate constant (k_{off}) of the NS3−Pep4AK complex. NS3 protease (2 μM) was incubated for 20 s in the presence of 20 μM Pep4AK. The preformed complex (25 μL) was then diluted into 2.5 mL of buffer (50 mM Tris, pH 7.5, 3 mM DTT, 2% CHAPS, and 50% glycerol) containing 19.2 μM substrate S2. The solution was automatically stirred and manually mixed for 5 s, after which the progress curve was recorded over a time period of 700 s. Instantaneous velocities were calculated from the progress curve by linear regression analysis performed on 120 data points collected at intervals of 0.5 s along the curve. The velocities thus obtained were plotted against time and eq 6 was fitted to the data. k_{off} was calculated from the fit.

are characteristic of one or both of the two tryptophan residues of the protease experiencing a more hydrophobic environment upon cofactor binding. The fluorescence increase was dependent on the presence of glycerol (not shown), which is in agreement with both the kinetic data and the CD data discussed above.

We used the increase in tryptophan fluorescence to determine the dissociation constant of the complex independently from the presence of substrate (Figure 5). The K_d value thus obtained (6.8 μM) is in good agreement with the one determined kinetically (see above).

Pre-Steady State Kinetics of Complex Formation. We used the continuous cleavage assay of the fluorogenic ester substrate S2 previously described (Taliani et al., 1996) to monitor how progress curves are affected by addition of Pep4AK to the NS3 protease. The experiments have been performed using 19.2 μM initial substrate concentration (5 K_m). Under these conditions, 83% of the enzyme molecules will be present under the form of enzyme−substrate complexes ([E−S2]). The binding of Pep4AK to the NS3 protease under our experimental conditions can therefore be described as follows:

$$[E-S2] + [Pep4AK] \underset{k_{off}}{\overset{k_{on}}{\rightleftharpoons}} [Pep4AK-E-S2] \quad (7)$$

where [Pep4AK−E−S2] is the ternary enzyme−substrate−activator complex and k_{on} and k_{off} are the association and dissociation rate constants, respectively.

Progress curves in the absence (curve C), after preincubation (curve A), and upon addition of Pep4AK (curve B) are shown in Figure 6. From the time-dependence of the onset of activation, a first-order rate constant k_{obs} can be calculated, which is related to k_{on} and k_{off} according to eq 5. k_{obs} was determined at different Pep4AK concentrations, and k_{on} was calculated from a secondary plot of k_{obs} versus [Pep4AK] (not shown). From the slope of this plot we obtained $k_{on} = 390$ M^{-1} s^{-1}. k_{off} can be calculated from the intercept of the linear regression function with the *y*-axis. In this case, we obtained $k_{off} = 0.0015$ s^{-1}. Since this procedure used to calculate k_{off} may be affected by a rather large error, we undertook an independent determination of the dissociation rate constant by preforming an NS3−Pep4AK complex at high concentration, followed by dilution of the complex in a buffer-containing substrate. The velocity of catalysis was then monitored over a period of 700 s. Its decrease with time is expected to reflect the dissociation of the enzyme−activator complex. A plot of velocity versus time describing this behavior is shown in Figure 6. Subsequently, k_{off} was calculated from triplicate experiments and found to be 0.003 s^{-1}. From these values of k_{on} and k_{off}, K_d values could be calculated and found to be between 3.8 and 7.7

μM. These figures are in good agreement with the K_d values determined under equilibrium conditions.

DISCUSSION

The mechanism of activation of the NS3 protease by its cofactor NS4A is unknown. *In vivo* NS4A, besides exerting effects on the enzymatic activity of the protease, was also shown to stabilize it toward proteolytic degradation and to target the enzyme to cell membranes (Tanji et al., 1995). The latter function is probably linked to the N-terminal region of NS4A, spanning residues 1−21, which has been suggested to form a trans membrane helix. A clue to explain the stabilization effect is given by the recently published three-dimensional structure of the NS3−NS4A−peptide complex (Kim et al., 1996), in which the peptide is embedded in a β-sheet structure of the protease core, adopting approximately the same location as strand D1 in chymotrypsin. In the structure without NS4A, the N-terminus of the protease adopts an open conformation binding to hydrophobic surfaces of adjacent molecules in the asymmetric unit (Love et al., 1996). These data suggest that NS4A is an integral part of the enzyme and that its absence is likely to destabilize the protein. Still, it is not clear whether the orientation of the N-terminus in the structure without NS4A results from crystal packing or reflects the situation in solution. We have shown that the far-UV CD spectrum is not affected by complex formation with Pep4AK, suggesting that no major rearrangements in the secondary structure of the enzyme occur upon binding to the cofactor, which is at variance with the crystal data. Our determination of the secondary structure of NS3 in solution was 10% helix, 38% β structure, and 52% other structures. This analysis shows a much better agreement with the one derived from the three-dimensional structure of NS3−NS4A complex (11% helix, 43% β structure, and 46% other structures) rather than with the one of NS3 alone (3% helix, 47% β structure, and 50% other structures). Also, we were unable to detect a deviation from monomeric state of NS3 in the absence of Pep4AK (data not shown). Our hypothesis is that the N-terminus of the uncomplexed protease is not disordered and exhibits the same secondary structure as in the complex. However, in the absence of Pep4AK it might still be endowed with quite a large conformational freedom. Being not optimally packed and very hydrophobic, this region might be stabilized in the crystal *via* intermolecular interactions that do not occur in solution.

We have shown that complex formation is modulated by the physicochemical conditions under which it is monitored. In particular, we have found that glycerol (and to a lesser degree also the detergent CHAPS) is a requirement for binding to the cofactor. Glycerol is known to have stabilizing effects on proteins that have been explained by its stronger solvophobic effect as compared to acqueous solvents (Timasheff, 1993). Also, dimer stabilization by glycerol has recently been shown for viral proteases such as CMV protease (Darke et al., 1996; Margosiak et al., 1996; Cole, 1996). In our case, we have found that glycerol increases the overall intensity of the near-UV CD spectrum. This increase is expected to reflect differences in side chain packing.

On the other hand, complex formation with Pep4AK causes a decrease of the intensity of the CD band in the region between 270 and 290 nm. This finding could be explained by the cancelling of negative and positive CD signals arising by the conformational transition of the side chains. Alternatively, it could be assumed that some tyrosines and/or tryptophans could have become more exposed to solvent and quite mobile as a consequence of complex formation. This latter hypothesis, however, is unlikely for the two tryptophan residues, because of the results obtained by fluorescence spectroscopy. In fact, under the same conditions, tryptophan fluorescence spectra show a blue shift and a concomitant increase in intensity. Taken together, the spectroscopic data suggest that one or both of the protein tryptophan residues are shifted into a more hydrophobic environment. In the structure of the NS3−Pep4A complex, the side chain of Val23 of the NS4A peptide is buried in a hydrophobic pocket at the bottom of which Trp85 is located. As a consequence, this tryptophan residue is expected to experience major differences in its physicochemical environment upon Pep4AK binding and is therefore the most likely candidate to which the changes in both CD and fluorescence spectra can be ascribed. These findings can be directly correlated with the activation mechanism of the NS4A cofactor. We have shown that the free protease is active *per se*, although to about a 7-fold lower degree. The extent of activation depends on the sequence of the substrate (Urbani et al., 1997) and is restricted to an increase in k_{cat}, at least using substrate S1. The rate-limiting step in amide bond hydrolysis by serine proteases usually is the acylation of the serine nucleophile at the enzyme's active site. Conversely, during ester bond scission by serine proteases, acylation is usually fast, with deacylation of the enzyme becoming the rate-limiting step (Fersht, 1985). We have previously shown that deacylation is indeed rate limiting in the hydrolysis of ester substrates based on the sequence of the NS4A/NS4B cleavage site as documented by a decrease in the K_m value with respect to the homologous amide substrates (Bianchi et al., 1996; Urbani et al., 1997) and by characteristic burst kinetics (Urbani et al., 1997). Since an NS4A−peptide-induced increase in k_{cat} can be seen both on amide and on ester substrates activation appears to affect both acylation and deacylation rate constants.

Our hypothesis is that cofactor binding causes rearrangements in the active site leading to a realignment of the catalytic triad. This finds support in the comparison of the crystal structures with and without cofactor. In the latter, His57 is oriented toward the catalytic serine but is too far away to abstract a proton. Furthermore, Asp81, expected to provide charge stabilization for His57 after deprotonation of Ser139, is oriented away and forms an ion pair with Arg155. These features change in the complex with Pep4A, yielding an enzyme with a "conventional" catalytic triad. It appears that the distortion of the catalytic triad observed in the uncomplexed NS3 should yield an inactive enzyme or an enzyme that cleaves peptide bonds by a substantially different mechanism than that employed by the NS3−NS4A complex. This raises the question whether the activity observed in the absence of the cofactor is attributable to a homogeneous population of sparingly active enzyme molecules or whether in solution there is an equilibrium between inactive and fully active enzyme molecules that is influenced by both buffer composition and addition of Pep4AK. If such an equilibrium exists, it has to be fast since active site titrations performed on the enzyme in the absence of its cofactor have yielded 94% active sites (Urbani et al., 1997).

The effects of Pep4AK on tryptophan fluorescence and on enzymatic activity were used to determine the equilibrium dissociation constants of the complex. The values that we obtained by both methods were in the low micromolar range, a value which is unexpectedly high taking into account the number of contacts that link the two molecules in the complex and that lead to a total of 2400 Å^2 of buried surface area (Kim et al., 1996). To address this issue, we followed the association and dissociation kinetics of the complex. The on-rates of complex formation turned out to be very slow with $k_{on} = 390\ M^{-1}\ s^{-1}$. It has to be remarked that this value has been obtained in 50% glycerol, which is expected to impose limitations on diffusion rates due to increased viscosity. In fact, at the temperature of our experiments (20 °C), viscosity increases 7-fold when going from 0 to 50% glycerol (Dobrota & Hinton, 1992). Since there is an inverse relationship between the diffusion coefficient of a given molecule and the viscosity of the medium, viscosity effects are likely to decrease on-rates by not more than 1 order of magnitude. Glycerol has additional effects on the hydration properties of proteins (Timasheff, 1993) thereby potentially affecting Stoke's radii. However, the order of magnitude of these effects is such that they cannot account alone for the slow association rate of NS3 with its cofactor peptide. Therefore, it must be assumed that association with Pep4AK is limited by some slow transient rearrangement which is necessary to accomodate the cofactor productively within its binding site. Differently from the slow association rate, k_{off}, was relatively fast, leading to a complex half-life of about 3.5 min.

The stability measured for the complex between the protease domain and the NS4A peptide differs significantly from what has been observed for the complex between full-length NS3 and full-length NS4A. When this complex was formed by *in vitro* translation and immunoprecipitated at different times, no evidence of complex dissociation could be detected for up to 6 h, suggesting very long half-lives of the native complex (De Francesco, R., unpublished observations). Therefore, it is possible that other portions of either the NS4A or the full-length NS3 protein may contribute to complex stability.

ACKNOWLEDGMENT

We are grateful to R. Cortese for continuous support of this work, to V. G. Matassa for critical reading of the manuscript, to S. Acali for peptide synthesis, to R. Petruzzelli for N-terminal sequence analysis, and to F. Naimo for mass spectrometry.

REFERENCES

Andrade, M. A., Chacón, P., Merolo, J. J., & Morán, F. (1993) *Protein Eng. 6*, 383−390.

Bartenschlager, R. L., Ahlborn-Laake, L., Mous, J., & Jacobsen, H. (1993) *J. Virol. 67*, 3835−3844

Bartenschlager, R., Lohmann, V., Wilkinson, T., & Koch, J. A. (1995) *J. Virol. 69*, 7519−7528

Bianchi, E., Venturini, S., Pessi, A., Tramontano, A., & Sollazzo, M. (1994) *J. Mol. Biol. 236*, 649−659.

Bianchi, E., Steinkühler, C., Taliani, M., Urbani, A., De Francesco, R., & Pessi, A. (1996) *Anal. Biochem. 237*, 239−244.

Butkiewicz, N., Wendel, M., Zhang, R., Jubin, R., Pichardo, J., Smith, E., Hart, A., Ingram, R., Durkin, J., Mui, P., Murray, M., Ramanathan, L., & Dasmahapatra, B. (1996) *Virology 225*, 328−338.

Cha, S. (1976) *Biochem. Pharmacol. 25*, 2695−2702.

Cole, J. (1996) *Biochemistry 35*, 15601−15610.

Darke, P. L., Cole, J. L., Waxman, L., Hall, D. L., Sardana, M., & Kuo, L. C. (1996) *J. Biol. Chem. 271*, 7445−7449.

Dobrota, M., & Hinton, R. (1992) in *Preparative centrifugation, a practical approach* (Rickwood, D., Ed.) pp 77−142, Oxford University Press, Oxford.

Eckard, M. R., Selby, M., Masiarz, F., Lee, C., Berger, K., Crawford, K., Kuo, C., Kuo, G., Houghton, M., & Choo, Q. L. (1993) *Biochem. Biophys. Res. Commun. 192*, 399−406.

Failla, C., Tomei, L., & De Francesco, R. (1994) *J. Virol. 68*, 3753−3760.

Failla, C., Tomei, L., & De Francesco, R. (1995) *J. Virol. 69*, 1769−1777.

Fersht, A. (1985) *Enzyme Structure and Mechanism*, Freeman, New York.

Grakoui, A., McCourt, D. W., Wychowski, C., Feinstone, S. M., & Rice, C. M. (1993) *J. Virol. 67*, 2832−2843.

Hijikata, M., Mizushima, H., Tanji, Y., Komoda, Y., Hirowatari, Y., Akagi, T., Kato, N., Kimura, K., & Shimotohno, K. (1993) *Proc. Natl. Acad. Sci. U.S.A. 90*, 10773−10777.

Kahn, P. C. (1979) *Methods Enzymol. 61*, 339−378.

Kim, J. L., Morgenstern, K. A., Lin, C., Fox, T., Dwyer, M. D., Landro, J. A., Chambers, S. P., Markland, W., Lepre, C. A., O'Malley, E. T., Harbeson, S. L., Rice, C. M., Murcko, M. A., Caron, P. R., & Thomson, J. A. (1996) *Cell 87*, 343−355.

Koch, J. O., Lohmann, V., Herian, U., & Bartenschlager, R. (1996) *Virology 221*, 54−66.

Komoda, Y., Hijikata, M., Tanji, Y., Hirowatari, Y., Mizushima, H., Kimura, K., & Shimotohno, K. (1994) *Gene 145*, 221−226.

Lin, C., Pragai, B. M., Grakoui, A., Xu, J., & Rice, C. M. (1994) *J. Virol. 68*, 8147−8157.

Lin, C., Thomson, J. A., & Rice, C. (1995) *J. Virol. 69*, 4373−4380.

Love, R. A., Parge, H. E., Wickersham, J. A., Hostomsky, Z., Habuka, N., Moomaw, E. W., Adachi, T., & Hostomska, Z. (1996) *Cell 87*, 331−342.

Margosiak, S. A., Vanderpool, D. L., Sisson, W., Pinko, C., & Kan, C. C. (1996) *Biochemistry 35*, 5300−5307.

Mori, A., Yamada, K., Kimura, J., Koide, T., Yuasa, S., Yamada, E., & Miyamura, T. (1996) *FEBS Lett. 378*, 37−42.

Morrison, J. F. (1982) *Trends Biochem. Sci. 7*, 102−105.

Satoh, S., Tanji, Y., Hijikata, M., Kimura, K., & Shimotohno, K. (1995) *J. Virol. 69*, 4255−4260.

Shimizu, Y., Yamaji, K., Masuho, Y., Yokota, T., Inoue, H., Sudo, S., & Shimotohno, K. (1996) *J. Virol. 70*, 127−132.

Shoji, I., Suzuki, T., Chieda, S., Sato, M., Harada, T., Chiba, T., Matsuura, Y., & Miyamura, T. (1995) *Hepatology 22*, 1648−1655.

Steinkühler, C., Urbani, A., Tomei, L., Biasiol, G., Sardana, M., Bianchi, E., Pessi, A., & De Francesco, R. (1996a) *J. Virol. 70*, 6694−6700.

Steinkühler, C., Tomei, L., & De Francesco, R. (1996b) *J. Biol. Chem. 271*, 6367−6373.

Strickland, E. H. (1974) *CRC Crit. Rev. Biochem. 2*, 113−175.

Suzuki, T., Sato, M., Chieda, S., Shoji, I., Harada, T., Yamakawa, Y., Watabe, S., Matsuura, Y., & Miyamura, T. (1995) *J. Gen. Virol. 76*, 3021−3029.

Taliani, M., Bianchi, E., Narjes, F., Fossatelli, M., Urbani, A., Steinkühler, C., De Francesco, R., & Pessi, A. (1996) *Anal. Biochem. 240*, 60−67.

Tanji, Y., Hijikata, M., Satoh, S., Kaneko, T., & Shimotohno, K. (1995) *J. Virol. 69*, 1575−1581.

Timasheff, S. N. (1993) *Annu. Rev. Biophys. Biomol. Struct. 22*, 67−97.

Tomei, L., Failla, C., Santolini, E., De Francesco, R., & La Monica, N. (1993) *J. Virol. 67*, 4017−4026.

Tomei, L., Failla, C., Vitale, R. L., Bianchi, E., & De Francesco, R. (1996) *J. Gen. Virol. 77*, 1065−1070.

Urbani, A., Bianchi, E., Narjes, F., Tramontano, A., De Francesco, R., Steinkühler, C., & Pessi, A. (1997) *J. Biol. Chem. 272*, 9204−9209.

Williams, J. W., & Morrison, J. F. (1979) *Methods Enzymol. 63*, 437−467.

Woody, R. W. (1995) *Methods Enzymol. 246*, 34−71.

BI9631475